ЖУРНАЛ СТРУКТУРНОЙ ХИМИИ

2016. Том 57, № 1 *Январь – февраль* *С. 40 – 52*

UDC 541.6:546.621:546.73

GEOMETRIES, STABILITIES, ELECTRONIC, AND MAGNETIC PROPERTIES OF SMALL ALUMINUM CLUSTER ANIONS DOPED WITH COBALT: A DENSITY FUNCTIONAL THEORY STUDY

L. Zhang, C.-Y. Zhang, X.-H. Song, B.-Q. Wang, J. Zhang

School of Chemistry and Material Science, Shanxi Normal University, Linfen, P. R. of China
E-mail: zhangcy66@126.com

Received December, 27, 2014 *Revised March, 11, 2015*

The geometrical structures, relative electronic and magnetic properties of small Al_nCo^- ($1 \le n \le 9$) clusters are systematically investigated within the framework of density functional theory at the BPW91 level. The single Co doping can dramatically affect the ground state geometries of the Al_{n+1}^- clusters. At the same time, the resulting geometries show that the lowest energy Al_nCo^- clusters prefer to be three dimensional structures. Here, the relative stabilities are investigated in terms of the calculated average binding energies, fragmentation energies, and second-order energy differences. Moreover, the result of the highest occupied-lowest unoccupied molecular orbital energy gaps indicates that Al_6Co^- clusters have the highest chemical stability for Al_nCo^- ($1 \le n \le 9$) clusters. Furthermore, the natural population analysis reveals that the charges in Al_nCo^- clusters transfer from the Al frames to the Co atom. Additionally, the analyses of the local and total magnetic moments of the Al_nCo^- clusters show that the magnetic effect mainly comes from the Co atom.

DOI: 10.15372/JSC20160105

K e y w o r d s: aluminum-cobalt cluster, geometric structure, relative stability, electronic property, density functional theory.

INTRODUCTION

During the last two decades, numerous theoretical and experimental efforts have been devoted to studying the structural, electronic, optical, and magnetic properties of atomic clusters [1—5]. Because they may consist of identical atoms, or molecules, or two or more different species materials. The properties of atomic clusters are not only distinctly different from those of discrete molecules or bulk materials but also often change drastically with increasing cluster size. Therefore, the study of the structure of amorphous systems in relation to the cluster size is a prerequisite for the understanding of their special physical and chemical properties. Especially, as a typical example of atomic clusters, increased interest in the area of the physical and chemical properties of aluminum clusters has been a subject of many theoretical and experimental studies [6—10] due to their potential applications in microelectronics [11] and nanocatalysis [12]. For instance, small neutral and charged clusters of Al_n ($1 \le n \le 15$) have been explored theoretically [13—20] and experimentally [21—26]. Meanwhile, the experimental data and computational simulations show that the stability of 20-electron Al_7^+ and 40-electron Al_{13}^- can be explained by a shell closure predicted by the jellium model because Al valence electrons have the free-electron-like behavior [27, 28].

Recently, much attention has been paid to doped aluminum clusters. Among various doped Al clusters, those doped with transition metals (TMs) have been in focus [29—34]. To some extent because of certain special and potential applications of mixed clusters in many fields, such as high-density magnetism recording, catalysis, optics, and biomedical aspects, a larger number of theoretical and experimental investigations improve the understanding of their structures, electronic and magnetic properties. In terms of the prominent transition metal element (cobalt), numerous theoretical and experimental efforts have been devoted to study the structural, electronic, magnetic, and other properties [35—42]. For instance, the electronic structures and magnetism of the neutral Al_nCo ($1 \le n \le 12$) cluster have been reported by Mei Wang *et al.* [35]. Moreover, several years ago Nonose *et al.* [37] performed chemisorption reactivity studies of neutral Al_nCo_m ($n > m$) and Co_nAl_m ($n > m$) clusters toward H2 using fast flow reactors. Knickelbein and co-workers [38, 39] succeeded in a comprehensive investigation of the size dependence of ionization potentials (IPs) of these clusters. These IP studies show that the electronic shell structure of Al_nCo and Al_nCo_2 clusters remains similar to that of pure Al_n clusters. Especially, Morse and co-workers [40] have performed resonant two-photon ionization spectroscopy on small diatomic AlCo aluminides. Above more, bimetallic aluminum cobalt cluster anions were studied by Axel Pramann and Atsushi Nakajima by photoelectron spectroscopy [44]. They extend the investigations on the aluminum cobalt cluster systems by probing the electronic structure of mass-selected negatively charged $Al_nCo_m^-$ and $Co_nAl_m^-$ clusters (*n.m*) in the near of the electron threshold binding energy(BE) using photodetachment photoelectron spectroscopy (PES). However, very little computational work has been devoted so far to the research on the geometries, stability, electronic and magnetic properties of small Al_nCo^- ($1 \le n \le 9$) clusters, but for the interesting progression established by in [43, 45]. We have not yet fully understand how the optimal structures and the stability change with cluster composition; how the nature of binding between Co and Al atoms changes when more Al atoms are added. Under this background, in order to further understand the properties of Al_nCo^- clusters, it is necessary for us to study the structures and physical or chemical properties of small aluminum cluster anions doped with cobalt and Al_nCo^- ($1 \le n \le 9$) clusters are expected to possess the unique structure and electronic as well as magnetic properties.

The reason why the research of the most stable structures of bimetallic clusters remains a challenge is that there is a huge amount of possible isomers. More importantly, if one metal is magnetic, the study becomes more complicated because several spin states must be considered and in troubles of the current restricted computational power, the lowest energy isomer is easy to miss. In this paper, we chose the Al_nCo^- clusters up to ten atoms and systematically investigated the structures, electronic and magnetic properties of Al_nCo^- ($1 \le n \le 9$) clusters based on the density function theory. Our main objectives of the present work were to identify the most stable structures and magnetic coupling natures of the Al_nCo^- cluster, to disclose how the electronic structure of the doped alloy cluster impacts the magnetic property, and finally to provide a comprehensive understanding of Al_nCo^- clusters. We hope that the results of our research will enlighten the further experimental and theoretical studies.

THEORETICAL METHODS AND COMPUTATIONAL DETAILS

All calculations of Al_{n+1}^- and Al_nCo^- clusters were performed by means of the density function theory (DFT) method provided in the GAUSSIAN 03 programs. To obtain the global minimum structures of Al_nCo^- clusters, a large variety of possible geometrical arrangements of these clusters were investigated, including three dimensional (3D), planar, cyclic, and linear configurations where n aluminum and one cobalt atoms are placed in different ways where they can group. The geometry optimization of Al_{n+1}^- and Al_nCo^- clusters are carried out with the exchange correlation function combining Becke′s exchange [46] with Perdew-Wang′s correlation functionals [47], referred to as BPW91 and the 6-311+G(2*d*) basis set. As for the accuracy and consistency, the exchange correlation function on mixed metal clusters has been fully tested by the previous publications [1, 2]. According to them, the geometries of all the clusters obtained within different functions are essentially identical. The 6-311+G(2*d*) basis set was used for both Co and Al atoms. The reliability of the present computational

Table 1

Bond lengths R, Å *and binding energies* BE, eV *of* Al_2 *and* Co_2 *dimers*

Dimer	*R*	BE	Dimer	*R*	BE
	Co_2			Al_2	
Present work	1.98	1.16	Present work	2.49	1.56
Other work [51]	2.12	2.74	Other work [52]	2.76	0.65
Experiment	2.31 [49]	Less than 1.32 [50]	Experiment [48]	2.47	1.50

scheme was validated by performing calculations of Al_2 and Co_2 dimers and by comparing the theoretical results with the experimental ones summarized in Table 1. The bond length (2.49 Å) and binding energy (1.56 eV) of Al_2 are good in agreement with the experimental values of 2.47 Å and 1.50 eV [48], respectively. Meanwhile, the calculated results of Co_2 show the bond length of 1.98 Å and the binding energy of 1.16 eV. Experimentally, Co_2 was first studied by Kant and Strauss by mass spectrometric techniques and a binding energy of 1.72 eV as well as a bond length of 2.31 Å were derived [49]. However, a more recent estimate of the binding energy by CID gave a value of less than 1.32 eV [50]. Our calculated bond length of Co_2 is slightly shorter than the research results of Kant and Strauss while the binding energy is in nice accordance with the experimental data (1.32 eV). At the same time, the BSSE energy of Co_2 is only 0.019 eV, the effect of which is so small that can be neglected. It is well known that the reliability of DFT studies determined by the choice of the functional and the basis set for the problem under investigation. Thus, the comparison reveals that the BPW91 functional and the 6-311+G(2*d*) basis set are optimal. Moreover, in order to get more reliable results, it is necessary to considered a more accurate CCSD(T) method. The CCSD(T) method was only used to study the single point energies of Al_nCo^- ($1 \le n \le 6$) clusters in Fig. 1. Fortunately, the energy change trend of Al_nCo^- clusters from one to six is basically the same, according to the CCSD(T) and BPW91 data. Especially, the corresponding global minimum structures of Al_nCo^- ($1 \le n \le 6$) clusters calculated by CCSD(T) are completely consistent with those calculated by the BPW91 method. Therefore, the BPW91 method can be applied to the bimetallic aluminum cobalt cluster.

Those amounts of possible initial structures of Al_{n+1}^- and Al_nCo^- ($1 \le n \le 9$) clusters are optimized with various spin multiplicity, and the one which has the lowest energy and low-lying isomers are shown in Fig. 1. Vibrational frequencies were also analyzed to confirm the stability of the structure. Here, all of the structures reported have positive vibrational frequencies. Moreover, in our optimizations the total energies of these lowest energy clusters are then used to study the evolution of their first vertical electron detachment energies (VDE = $E_{\text{neutral at optimized anion geometry}} - E_{\text{optimized anion}}$), average binding energy (E_b), fragmentation energies, and second-order energy differences as a function of the cluster size. All charge populations were obtained by the natural population analysis (NPA) [53, 54]. To identify the most stable cluster, E_b was calculated from

$$E_b(Al_nCo^-) = \frac{nE(Al) + E(Co^-) - E(Al_nCo^-)}{n+1}, \quad (1)$$

where E(Al), E(Co^-), E(Al_nCo^-) are the total energies of the Al atom, Co^- anions, and the Al_nCo^- cluster, and

$$E_b(Al_{n+1}^-) = \frac{nE(Al) + E(Al^-) - E(Al_{n+1}^-)}{n+1}, \quad (2)$$

where E(Al), E(Al^-), and $E(Al_{n+1}^-)$ represent the total energies of the lowest energy atoms or clusters for Al, Al^-, and Al_{n+1}^-, respectively.

The common HOMO—LUMO gap (GAP) is computed as the energy difference between the highest occupied molecular orbital and the lowest unoccupied molecular orbital. There is no doubt that GAP as an important indicator of the relative stability can to some extent reflect the ability of the

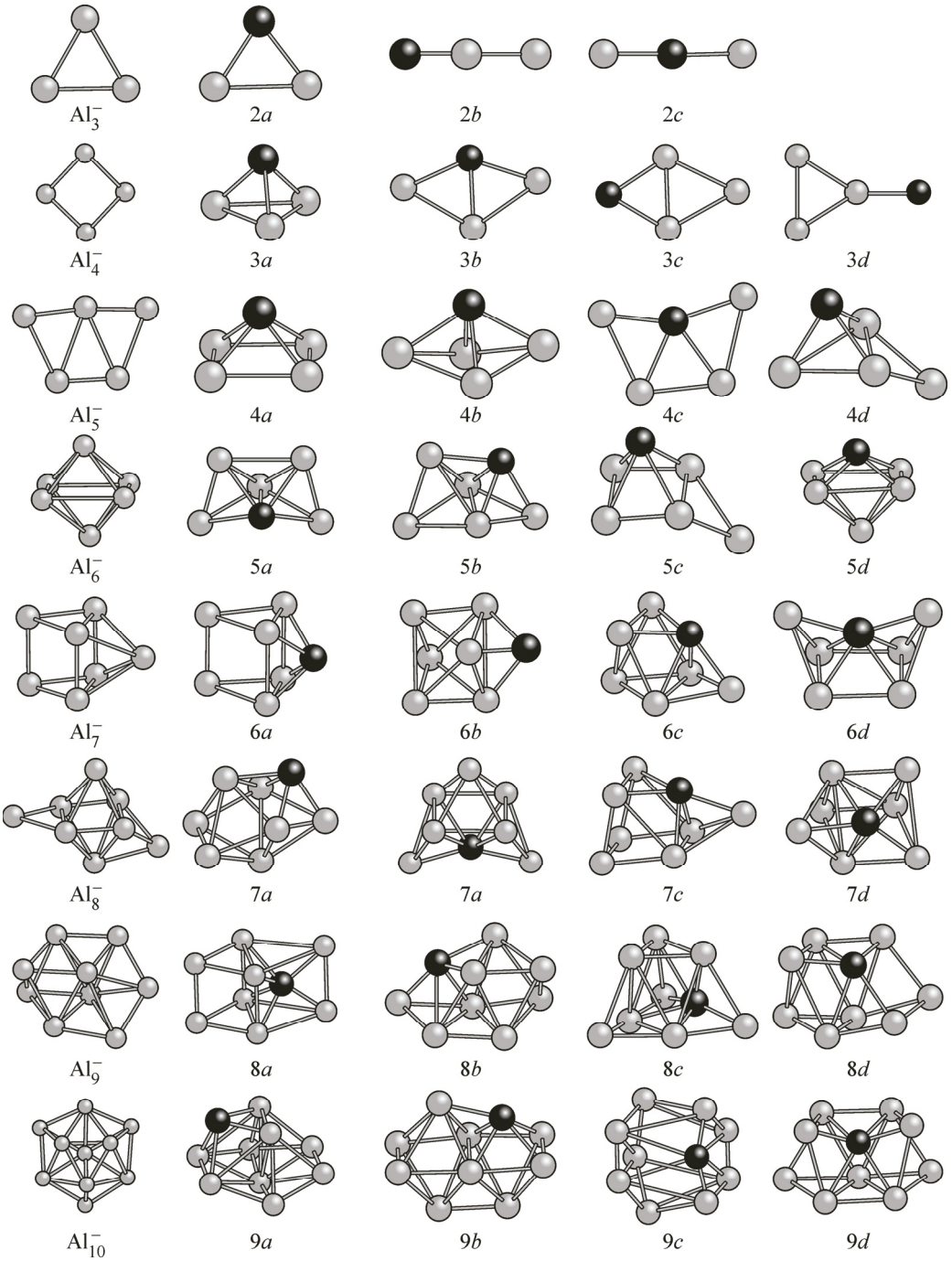

Fig. 1. Lowest energy structures and low-lying isomers for Al_nCo^- ($1 \le n \le 9$) clusters, and the ground state structures of pure aluminum clusters Al_{n+1}^- ($1 \le n \le 9$) are listed on the left. The brown and blue balls represent the Al and Co atoms, respectively

molecule to participate in chemical reactions. Thus, the HOMO—LUMO gaps of the most stable isomers were also obtained by the BPW91 method with the 6-311+G(2*d*) basis set. The second-order energy differences were calculated as shown below:

$$\Delta_1 E(Al_nCo^-) = E(Al_{n-1}Co^-) + E(Al) - E(Al_nCo^-), \quad (3)$$

$$\Delta_2 E(Al_nCo^-) = E(Al_{n-1}Co^-) + E(Al_{n+1}Co^-) - 2E(Al_nCo^-), \quad (4)$$

where E(Al), E(Co^-), E(Al_nCo^-), E($Al_{n1}^-Co^-$) and E($Al_{n+1}Co^-$) are the total energies of the most stable Al, Co^-, Al_nCo^-, $Al_{n1}^-Co^-$ and $Al_{n+1}Co^-$ clusters.

RESULTS AND DISCUSSION

A large number of possible structures of Al_nCo^- ($1 \le n \le 9$) clusters were optimized at the DFT/BPW91/6-311+G(2*d*) level to obtain the corresponding global minimum structures. The CCSD(T) method with the 6-311+G(2*d*) basis set proved that the global minimum structures were reliable. However, we present only the results about the four lowest energy structures for different-size clusters in Fig. 1. According to the total energy from low to high, different low-lying isomers are defined by *na*, *nb*, *nc*, and *nd*, where *n* is the number of Al atoms in Al_nCo^- clusters. The optimized spin multiplicities, symmetries, relative energies, average nearest neighbor distances between the aluminum atoms and the cobalt atom, natural charge populations (NCPs) as well as the enthalpy of formation to validate the stability of the clusters are displayed in Table 2. Relative energies are the total energies between the lowest energy structures and low-lying isomers of Al_nCo^- ($1 \le n \le 9$) clusters. Enthalpies of formation are calculated as

$$\Delta H = \frac{H(Al_nCo^-) - nH(Al) - H(Co^-)}{n+1},$$

where H(Al), H(Co^-), H(Al_nCo^-), H($Al_{n-1}Co^-$), and H($Al_{n+1}Co^-$) are the thermal enthalpies of the most stable Al, Co^-, and Al_nCo^- clusters.

Equilibrium geometries and vertical detachment energies. For the equilibrium geometries of $AlCo^-$ ($C_{\infty v}$), we found the ground state to be an $S = 2$ state with a bond length of 2.26 Å that is shorter than that of Al_2^- (2.59 Å) and a bond energy of 2.43 eV that is smaller than that of the Al_2^- cluster (2.56 eV). The BSSE energy of the $AlCo^-$ cluster is 0.04 eV (1.8 %). It is so small that we can ignore its effect. Since no experimental results to support the reasonableness of the doped $AlCo^-$ cluster have been obtained so far, we calculated all VDEs for the lowest energy structures of Al_nCo^- as well as Al_n^- clusters from $n = 1$ to $n = 9$. Here, the calculated VDE result of $AlCo^-$ is 1.10 eV, and the value for Al_2^- is 1.30 eV, which is slightly less than the experimental data of 1.46±0.01 eV [26].

All possible initial structures of the Al_2Co^- cluster, i.e., linear ($D_{\infty h}$,$C_{\infty v}$) and triangular structures, are optimized at the BPW91 level. The calculations illustrate that isosceles triangular isomer 2a with the C_{2v} symmetry is the ground state structure of Al_2Co^-, the corresponding electronic state is triplet state $^3A_1$, with two Al—Co bond lengths of 2.28 Å, Al—Al bond lengths of 2.61 Å, and an apex angle of 69.8°. It is lower than linear structures 2b and 2c by 1.32 eV and 1.35 eV. In fact, the most stable pure aluminum cluster Al_3^- is found to be an equilateral triangle of the quartet state with a bond length of 2.53 Å in accordance with the previous data (2.54 Å) [52]. Furthermore, our calculated VDE is 1.30 eV for the ground state structure of the Al_2Co^- cluster, whereas calculated VDE is 1.70 eV for the Al_3^- cluster, which is in agreement with the experimental data of 1.89±0.04 eV [26].

The initial trial geometries considered for the tetramer Al_4^- clusters are tetrahedral, rhombic, square, and butterfly-like structures. The ground state structure of Al_4^- is a planar rhombic structure, which agrees with the recent theoretical study [52]. In the bimetallic Al_3Co^- clusters, most stable structure 3a together with other three different low-lying isomers 3b, 3c, and 3d is achieved within an energy range of 1.86 eV. The calculated result reveals that doublet state ($^2A_1$) isomer 3a (C_{3v}) with three equal Al—Co bond lengths (2.26 Å), three equal Al—Al distances (2.75 Å) is lower in total energy than 3b, 3c, and 3d by 1.04 eV, 1.42 eV, and 1.86 eV. The average nearest-neighbor Al—Co distance (2.36 Å) in irregular quadrilateral 3b is longer than that of lowest energy isomer 3a, showing the reduced stability of isomer 3b relative to 3a. Rhombic isomer 3c is another stable configuration with the average Al–Co bond length of 2.33 Å. As compared to 3b, they both have the same C_{2v} symmetry. However, each has its own electronic state so that the most stable structures of 3b and 3c exist in the quartet and doublet states, respectively. The least stable structure in Al_3Co^- provided in Fig. 1 is

Table 2

Geometries, *spin multiplicities*, *symmetries*, *relative energies* (≥*E*), *enthalpy of their formation*, *average nearest neighbor distances between the aluminum atoms and the cobalt atom*. HOMO—LUMO (GAP) *and natural charge populations* (NCPs) *of the* Co *atom for* Al_nCo^- ($1 \le n \le 9$)

Isomer	Spin	Sym	≥*E*, eV	$R_{Al—Co}$, Å	GAP, eV	NCP	≥*H*, Kcal/mol
1a	2	$C_{\infty v}$	0.00	2.26	0.98	–0.671	–28.06
2a	3	C_{2v}	0.00	2.28	1.14	–0.323	–41.62
2b	3	$C_{\infty v}$	1.32	2.28	0.45	–0.407	–31.20
2c	5	$D_{\infty h}$	1.35	2.29	0.66	–0.229	–31.14
3a	2	C_{3v}	0.00	2.26	0.67	–0.758	–50.71
3b	4	C_{2v}	1.04	2.36	0.84	–0.278	–44.72
3c	2	C_{2v}	1.42	2.33	0.56	–0.332	–42.52
3d	6	C_{2v}	1.86	2.37	0.54	–0.036	–35.05
4a	3	C_{4v}	0.00	2.37	0.94	–0.597	–52.28
4b	5	C_2	0.89	2.41	0.56	–0.332	–48.19
4c	3	C_{2v}	1.05	2.35	0.72	–0.743	–47.43
4d	5	C_s	1.15	2.31	1.05	–0.367	–46.98
5a	2	C_s	0.00	2.44	0.57	–0.591	–52.05
5b	4	C_s	0.15	2.38	0.60	–0.519	–51.50
5c	2	C_s	0.27	2.36	0.66	–0.521	–51.02
5d	4	C_{4v}	0.32	2.33	0.20	–0.111	–51.14
6a	3	C_2	0.00	2.36	1.42	–0.334	–55.70
6b	3	C_s	0.28	2.36	1.44	–0.090	–54.78
6c	3	C_s	0.29	2.46	0.92	–0.423	–54.74
6d	1	C_{2v}	0.35	2.69	0.58	–1.166	–54.29
7a	2	C_s	0.00	2.34	0.55	–0.447	–56.84
7b	2	C_s	0.12	2.39	0.54	–1.007	–56.51
7c	2	C_s	0.19	2.35	0.82	–0.866	–56.29
7d	2	C_s	0.21	2.36	0.73	–0.850	–56.24
8a	1	C_{2v}	0.00	2.33	0.74	–1.486	–56.88
8b	3	C_1	0.06	2.39	0.62	–0.628	–56.72
8c	3	C_s	0.07	2.41	0.53	–0.931	–56.69
8d	1	C_s	0.10	2.43	0.54	–0.659	–56.61
9a	2	C_s	0.00	2.37	0.63	–0.337	–57.84
9b	2	C_s	0.08	2.39	0.56	–0.641	–57.67
9c	2	C_s	0.20	2.47	0.55	–0.870	–57.43
9d	2	C_{2v}	0.36	2.37	0.56	–1.207	–57.03

Y-shaped isomer 3d, which is 1.86 eV higher than isomer 3a. Obviously, it is the first time that the three dimensional (3D) shape for Al_nCo^- has appeared at $n = 3$. The calculated VDE value for isomer 3a is 1.43 eV. Meanwhile, theoretical VDE for Al_4^- is 2.19 eV, which is consistent with the experimental result (2.20±0.05 eV) [26].

The 3D irregular trapezoid structure with the C_s symmetry is the lowest one in energy for the Al_5^- cluster. It should be pointed out that the planar structure with the C_{2v} symmetry presented in [52] is a transition state in our optimization process, not corresponding to the potential energy minima. We have achieved lower energy Al_4Co^- clusters by either adding one Al atom to different Al_3Co^- isomers or exchanging one Al atom for one Co atom. Fortunately, after adding one Al atom to ground state 3a of Al_3Co^-, the most stable square pyramidal structure (4a) was found to have the C_{4v} symmetry and the

corresponding electronic state $^3A_2$ with four identical Al—Co bonds (2.37 Å) and four identical Al—Al bonds (2.70 Å). Isomer 4b with the C_2 symmetry is the energetically closest structure, which is 0.89 eV higher than that of lowest energy structure 4a. Planar ingot structure 4c with C_{2v} is generated when one Al atom in the lowest energy structure of Al_5^- is replaced by the Co atom, which is energetically higher than that of ground state structure 4a by 1.05 eV. Least stable structure 4d with the average nearest-neighbor distance of 2.31 Å for Al—Co is lower in energy than isomer 4a by 1.15 eV. In light of the calculated results, the VDE value is 2.05 eV of isomer 4a whereas VDE of the pure aluminum cluster Al_5^- is 2.14 eV, which is in good qualitative agreement with the experimental result (2.25±0.05eV) [26].

We performed an extensive computational research for the lowest energy structures of Al_6^-. Excitingly, our results agree with the calculations of Sun *et al*. who predicted the tetragonal bipyramidal structure with the D_{3d} symmetry as the ground-state geometry [52]. With regard to the Al_5Co^- cluster, numerous possible initial geometries are optimized. According to the calculated results, lowest energy structure 5a is the C_s ingot structure with the average nearest-neighbor distance of 2.44 Å for Al—Co bonds. Energetically closest isomer 5b is obtained by adding one Al atom to the structure of 4b, which is a quartet state with the C_s symmetry, and is 0.15 eV higher in energy than 5a. Another structure 5c in Fig. 1 has the C_s symmetry with the doublet state. Isomer 5d can be viewed as one Al atom in the ground state structure of Al_6^- substituted by one cobalt atom. This structure with four identical Al—Co bonds (2.33 Å) and C_{4v} symmetry is higher in energy than that of isomer 5a by 0.32 eV. Moreover, we also calculated VDE (2.56 eV) of the ground state structure of the Al_6^- cluster; the value is in satisfactory agreement with the experimental value (2.63±0.06 eV) [26]. It can be noted that VDE of isomer 5a is 2.12 eV, which is lower than that of the Al_6^- cluster.

Similar to the previous calculated result [49], the optimization results show that the lowest energy structure of Al_7^-, with the C_{3v} symmetry, is marked by an atom capping a ‘″square″ face. The lowest energy structure of 6a with the C_2 symmetry can be regarded as the Co atom substituting for the Al atom on the ″square″ face of the Al_7^- cluster. Another isomer 6b with one capped Co atom on the distorted triangular prism is 2.36 eV higher in total energy than the ground state of 6a. Afterwards, we performed an extensive search for other isomers and found the following two stable isomers: 6c and 6d, whose energies are higher than those of isomer 6a by 0.29 eV and 0.35 eV, respectively. In addition, in our theoretical calculation, the VDE value (2.66 eV) of isomer 6a and 2.36 eV of Al_7^- are also obtained. Fortunately, calculated VDE of Al_7^- is in accordance with the experimental value (2.43+ +0.06 eV) [26].

The lowest energy configuration of Al_8^- can be obtained by capping two Al atoms on the peripheral sites of the deformed stable frame of Al_6^-. In light of the calculated results of the Al_7Co^- cluster, it is interesting to find four low-lying isomers with the same spin multiplicity and doublet state. Lowest energy structure 7a can be obtained by adding one Al atom and one Co atom into the same side of the ground state Al_6^- cluster. Isomers 7b and 7c have a similar structure, but different total energy and average nearest-neighbor Al—Co distance, as shown in Table 2. Subsequent structure 7d is energetically higher than isomer 7a by 0.21 eV. Meanwhile, calculated VDEs of 7a (2.31 eV) and Al_8^- (2.41 eV) are obtained.

Among the extensive trial geometries of Al_9^- and Al_8Co^- clusters that we calculated, the ground state structure of Al_9^- is acquired for Al_9^- (Fig. 1), which is consistent with the structure proposed by Sun *et al*. [52]. Apparently, lowest energy structure 8a with the C_{2v} symmetry was achieved by adding one Al atom above the structure of isomer 7b. Energetically closest isomer 8b can be regarded as the Al atom in the ground state structure of Al_9^- replaced by one Co atom. Structures 8c and 8d with the same C_s symmetry are energetically higher than isomer 8a by 0.07 eV and 0.10 eV, respectively. Furthermore, VDE value of 2.41 eV for isomer 8a is also obtained by theoretical calculations.

Table 3

Binding energies EB (eV) *of global minimum structures of the* Al_nCo^- *clusters obtained with the* 6-311+G(2*d*) *basis set*

Cluster	CCSD(T)	BPW91
2a	1.91	1.80
3a	2.07	2.20
4a	2.19	2.27
5a	2.06	2.26
6a	2.24	2.43

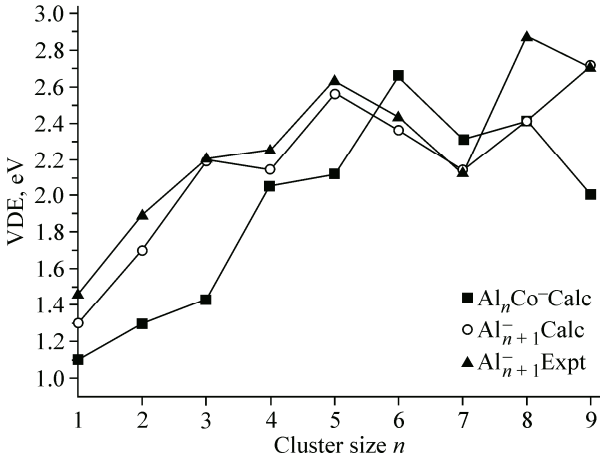

Fig. 2. Calculated and experimentally measured [26] vertical electron detachment energies (VDE) as a function of the cluster size

Finally, we present the equilibrium geometries of Al^-_{10} and Al_9Co^- clusters. According to the theoretical results of Al_9Co^- clusters, it can be observed that except for isomer 9d with the C_{2v} symmetry, lowest energy isomer 9a and two other low-lying isomers 9b and 9c possess the same geometrical C_s symmetry. And, more remarkable, all of four low-lying isomers shown in Fig. 1 have the same doublet state. In respect of energy, ground state structure 9a is lower than other three low-lying isomers 9b, 9c, and 9d by 0.08 eV, 0.20 eV, and 0.36 eV, respectively. Based on the calculated results, the VDE value of 2.70 eV for isomer 9a is very close to that of 2.71 eV for pure aluminum cluster Al^-_{10}, which is in good qualitative agreement with the experimental result (2.70+0.07 eV) [26].

According to the above discussion, although the lowest-energy configurations upon Al_nCo^- ($1 \le n \le 9$) and Al^-_{n+1} ($1 \le n \le 9$) clusters prefer the lowest spin state, the difference between them still demonstrates that the doped Co atom can dramatically affect the ground state geometries of the pure Al^-_{n+1} clusters. It is worth nothing that the doped Co atom tends to occupy the surface of the clusters.

The size effect on the computed VDE values for both Al_nCo^- and Al^-_{n+1} clusters as well as the experimentally measured [26] VDE results for Al^-_{n+1} clusters was plotted in Fig. 2. Despite a slight deviation of Al^-_9, the VDE values for Al^-_{n+1} clusters calculated by the BPW91 method and the trend of the obtained result was mainly consistent with that obtained in the experiment [26]. We suppose the reason for the deviation between our calculated VDE values and the experimental data to be the following several aspects. First of all, from the experimental point of view, the measured VDE value for the Al^-_9 cluster may be the result of the overlap of multiple structural isomers. Secondly, on the theoretical side, popular BPW91 and B3LYP methods regarded as the effective tools for the research of metallic clusters were applied to calculate the VDE value for the Al^-_9 cluster. At the 6-311+G(2*d*) level, the determined VDE values are 2.45 eV and 2.39 eV, both of which are slightly smaller than the experimental data of 2.85±0.08 eV. A more accurate method combined with a bigger basis set may be helpful for the investigation of the Al^-_9 cluster. Finally, we could not exclude the presence of the lower energy structure. Unfortunately, there are no experimental data on VDE for Al_nCo^- ($1 \le n \le 9$) at present. Of course, we hope it is useful to apply our theoretical data to guide further experiments on the determination of VDE values for Al_nCo^- ($1 \le n \le 9$).

Relative stability. In order to understand the relative stability and size-dependent behavior, the average binding energies for Al_nCo^- and Al^-_{n+1} cluster anions, as well as the fragmentation energies and second-order energy differences of Al_nCo^- clusters are investigated using the above formulas. The binding energies (E_b) of the global minimum structures of Al_nCo^- ($1 \le n \le 6$) clusters are compared in Table 3 using CCSD(T) and bpw91 functions in combination with the 6-311+G(2*d*) basis set and we find that they have a similar varying tendency. Meanwhile, according to Table 2, the values of the

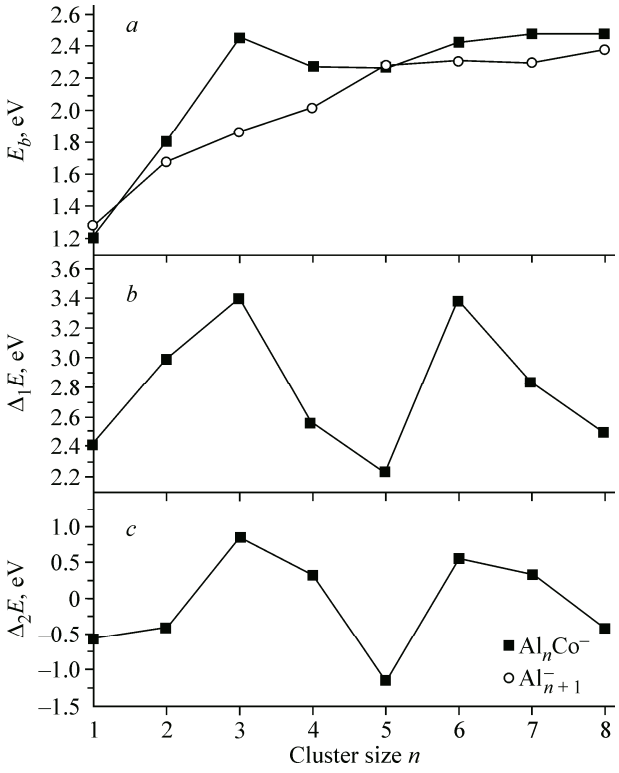

Fig. 3. Average binding energies for the lowest energy structures of Al_nCo^- and Al^-_{n+1} isomers as a function of the cluster size (*a*), size dependence of the fragmentation energies (*b*) and the second order energy differences (*c*) for the lowest energy structures of the Al_nCo^- clusters

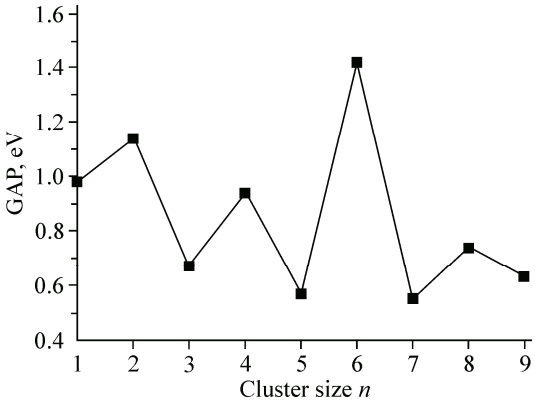

Fig. 4. Size dependence of the HOMO—LUMO gaps for the lowest energy structures of the Al_nCo^- clusters

enthalpy of formation in Fig. 2 are negative. Especially, the results of the enthalpy of formation show that their relative stability remains decreased from a to d. From Fig. 3 it is seen that the average binding energy of Al_nCo^- and Al^-_{n+1} cluster anions increases with increasing cluster size and it is seems that the average binding energies of Al_nCo^- clusters have higher binding energies than pure Al^-_{n+1}. This indicates that the doping of cobalt atom helps to improve the stability of the Al^-_n cluster. Moreover, a local binding energy peak appears at $n = 3$ and $n = 6$, implying that Al_3Co^- and Al_6Co^- clusters are more stable than the neighboring clusters.

Furthermore, the size dependence of the fragmentation energies and second order energy differences for Al_nCo^- ($1 \le n \le 9$) clusters are plotted in parts b and c of Fig. 3. It has been observed that the local peaks of the fragmentation energies and second order energy differences appear at $n = 3$ and $n = 6$, which indicates that Al_3Co^- and Al_6Co^- clusters are relatively more stable than the other isomers. This is the same that has been provided for the average binding energy, which also means that Al_3Co^- and Al_6Co^- clusters are more stable than their neighbors. On the contrary, both curves of the fragmentation energies and second order energy differences suddenly reach the minimum at $n = 5$, indicating that the Al_5Co^- cluster is the least stable structure among all investigated Al_nCo^- ($1 \le n \le 9$). As a final note, the maximum of our calculated VDE results appears at $n = 6$, which conforms to the result of fragmentation energies and second order energy differences.

Electronic properties. The HOMO—LUMO gap is a characteristic quantity of the electronic structure of clusters and also a measure of the ability for clusters to undergo activated chemical reactions with small molecules. Generally speaking, a larger gap indicates a weaker chemical activity, whereas a smaller one corresponds to a stronger chemical activity. The results of the HOMO—LUMO gap (GAP in eV) for the most stable clusters and low-lying isomers in their own spin states are presented in Table 2. The difference between the LUMO and HOMO eigenvalues for the lowest energy Al_nCo^- ($1 \le n \le 9$) clusters is shown in Fig. 4. Three apparent and significant characteristics are presented:

(a) the HOMO—LUMO energy gaps for the most stable geometries of Al_nCo^- clusters exhibit the odd-even oscillatory behavior from 1 to 9, indicating that even-numbered Al_nCo^- clusters are relatively more stable than their neighboring odd-numbered sizes;

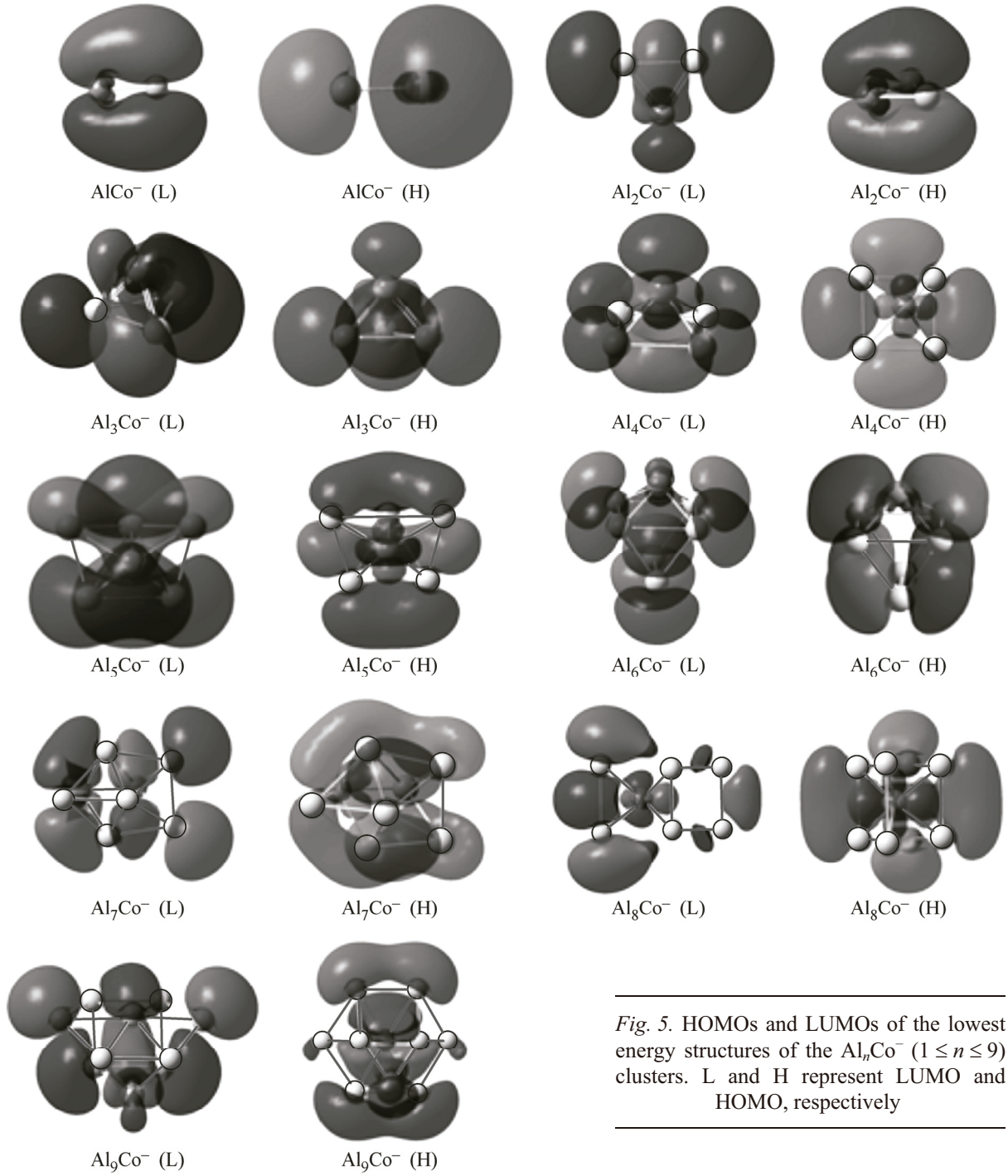

Fig. 5. HOMOs and LUMOs of the lowest energy structures of the Al_nCo^- ($1 \le n \le 9$) clusters. L and H represent LUMO and HOMO, respectively

(b) the HOMO—LUMO energy gap of the Al_nCo^- clusters reaches a maximum at $n = 6$, corresponding to a higher chemical stability of the Al_6Co^- cluster as compared to their neighbors. It is consistent with our calculated results of the average binding energy, fragmentation energy, and second-order energy difference for the Al_6Co^- cluster;

(c) the fact that the cluster size of $n = 3$ does not show as high stability as shown in Fig. 3, *b* and *c* is beyond expectation. This phenomenon may be a consequence of the energy gap calculation for open-shell systems, for which the energy gap is still in controversy because its HOMO is individually occupied and can easily accept or lose an electron.

To study the binding nature of Al_nCo^- clusters with reference to molecular orbitals, we have examined the density of states based on the contribution of different orbital components (*s*, *p*, *d*) and the electron density of the HOMO and LUMO states. Detailed analyses of electronic levels show that HOMOs and LUMOs of Al_nCo^- clusters mainly consist of 3*d*, 4*s*, and 4*p* states of the Co atom mixed with Al 3*s* and 3*p* states. The electron density distribution of HOMO and LUMO states of the most stable Al_nCo^- clusters is shown in Fig. 5. It is seen that all the HOMO and LUMO states are delocalized except the LUMO states of $AlCo^-$ and the HOMO states of the $AlCo^-$ cluster. Therefore, a change in the HOMO—LUMO gap caused by the doping Co atom should be attributed to the hybrid states.

To investigate the negative charge transfer within the clusters, we have performed the natural population analysis (NPA). All of the calculated NPA results of the Fe atom for the lowest and low-lying energy Al_nCo^- cluster are summarized in Table 2. As seen from the NPA calculation, the Co atom attracts 0.09—1.49 electrons from its neighboring Al atoms for the Al_nCo^- clusters. The charge transfer from the Al frames to the Co atom is in negative charges of the stable Al_nCo^- clusters, which indicates that the Al frames act as electron donors in all Al_nCo^- clusters. The reason for this phenomenon may be the higher electronegativity of the Co atom (1.88) than that of the Al atom (1.61). Meanwhile, Fig. 6 shows the natural charge population (NCP) of the most stable Al_nCo^- ($1 \le n \le 9$) clusters. It is seen that the Al frames in the $AlCo^-$, Al_3Co^-, Al_8Co^- clusters offer more electrons to share with the Co atom than their vicinity clusters. Especially, the Al frame shares charges with the Co atom in Al_8Co^- clusters, which implies that electronic interactions between the Co atom and the Al atom in Al_8Co^- clusters can be strongest. In order to investigate the internal charge transfer, the natural electron configuration of the impurity Co atom is also considered. In Table 3, the charges of the Co 3*d*, 4*s*, and 4*p* states in the lowest energy Al_nCo^- clusters are presented. For the Co atom, the 3*d* as well as 4*p* states respectively get 1.13—2.44 *e* and 0.01—0.15 *e* electrons while the 4*s* state loses 0.53—1.46 *e* electrons. In addition, the contribution from 4*d*, 5*s*, 5*p* states is nearly zero. Hence, it can be concluded that there are electron transfers from the 4*s* state to 3*d* and 4*p* states in the internal of the Co atom. Based on the above, one can draw a conclusion that there is the charge transfer not only from Al frames to Co atom but also in the interior electronic shell in the ground state Al_nCo^- clusters.

Magnetic properties. Based on the most stable geometries, the total magnetic moments of Al_nCo^- as well as the local magnetic moments of Co atoms in Al_nCo^- clusters are presented in Fig. 7. As seen from Fig. 7, the total magnetic moments of Al_nCo^- clusters as a function of the cluster size exhibit the dramatic odd-even alternative behavior. The local magnetic moments of Co atoms have the same tendency. At $n = 1$ and $n = 9$, the local magnetic moments of Co atoms are larger than the total magnetic moments of Al_nCo^- clusters, whereas at $n = 2$, 3, 4, 5, 6, and 7 the local magnetic moments of Co atoms are smaller than the total magnetic moments of the Al_nCo^- clusters.

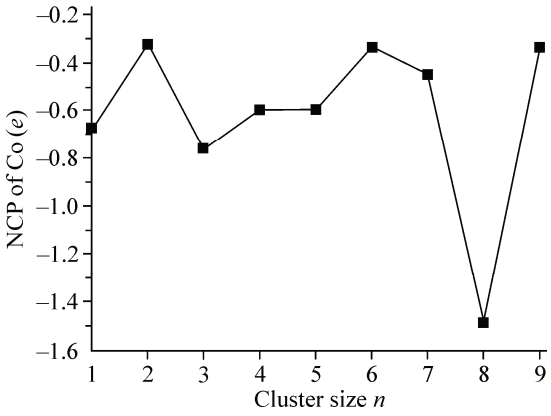

Fig. 6. Size dependence of the natural charge populations of the Co atom in the lowest energy structures of the Al_nCo^- ($1 \le n \le 9$) clusters

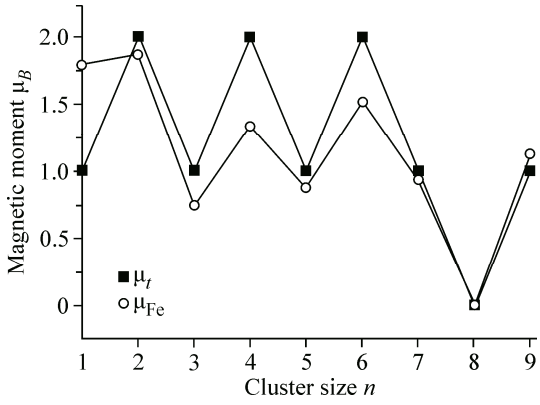

Fig. 7. Size dependence of the total magnetic moments of the Al_nCo^- clusters and the local magnetic moments on the Co atoms

Table 4

Total magnetic moment (μ_t) *of the* Al_nCo^- *clusters*, *local moment* (μ_{Co}) *of the* Co *atom*, *charge and local moments* (*in brackets*) *of* 3*d*, 4*s*, *and* 4*p states for the* Co *atom in the* Al_nCo^- ($1 \le n \le 9$) *clusters*

Cluster	μ_t	μ_{Co}	3*d*	4*s*	4*p*
$AlCo^-$	1.000	1.794	8.13 (1.732)	1.47 (0.083)	0.03 (–0.01)
Al_2Co^-	2.000	1.871	8.30 (1.469)	0.93 (0.145)	0.08 (0.027)
Al_3Co^-	1.000	0.740	8.80 (0.497)	0.80 (0.063)	0.11 (0.002)
Al_4Co^-	2.000	1.327	8.68 (1.045)	0.76 (0.079)	0.13 (0.004)
Al_5Co^-	1.000	0.870	8.82 (0.696)	0.61 (0.033)	0.15 (–0.00)
Al_6Co^-	2.000	1.517	8.53 (1.213)	0.68 (0.095)	0.12 (0.001)
Al_7Co^-	1.000	0.925	8.79 (0.743)	0.55 (0.042)	0.10 (0.000)
Al_8Co^-	0.000	0.000	9.44 (0.000)	0.81 (0.000)	0.01 (0.000)
Al_9Co^-	1.000	1.120	8.69 (0.914)	0.54 (0.055)	0.10 (0.000)

In order to gain more insights into the magnetic nature of the Al_nCo^- clusters, we implemented a detailed analysis of the onsite atomic charges and local magnetic moments of the Co atom. The magnetic moments (3*d*, 4*s*, and 4*p* states) for the Co atom in the Al_nCo^- clusters are presented in Table 4. All of the most stable Al_nCo^- ($1 \le n \le 9$) clusters, except for $n = 1$, 8, and 9, the total magnetic moment is mainly located on the Co atom. The magnetic moment of the Co atom is mainly from the 3*d* state; the 4*s* state and 4*p* state make no contribution to the magnetic moment of the Co atom. Thus, we can now say that 3*d* electrons have a great influence on the total magnetic moments of the Al_nCo^- clusters.

CONCLUSIONS

In summary, we have systematically studied the equilibrium geometries, relative stabilities, electronic and magnetic properties of different-size Al_nCo^- ($1 \le n \le 9$) clusters using DFT based on the BPW91 and CCSD(T) with the 6-311+G(2*d*) basis set. The lowest energy Al_nCo^- clusters have dissimilar geometries of Al_{n+1}^- clusters and the average binding energies of Al_nCo^- clusters are higher than those of pure Al_{n+1}^- clusters. In fact, the doping with a cobalt atom contributes to the stabilities of the aluminum clusters. For Al_nCo^- clusters, the 3D structure is more stable and the impurity Co atom prefers to reside at the surface of the clusters. The stability analysis in relation to the calculation of the average binding energies, fragmentation energies, second order energy differences indicates that Al_3Co^- and Al_6Co^- clusters possess a relatively higher stability. Moreover, the analysis of the HOMO—LUMO gaps and VDE reveals that the most stable configuration is Al_6Co^- clusters. Thus, we think that Al_6Co^- clusters have the highest stability among the Al_nCo^- ($1 \le n \le 9$) clusters. Furthermore, the result of NPA shows that there is not only the charge transfer from Al frames to the Co atom, but also the transfer from the 4*s* state to the 3*d* and 4*p* states in the interior electronic shell for the ground state Al_nCo^- clusters. Both local magnetic moment of the doped Co atom and total magnetic moments of the Al_nCo^- clusters show a pronounced odd-even oscillation when the cluster size increases. It must be pointed out that the total magnetic moment is mainly from the doped Co atom rather than Al_n^- clusters, and what is more important is that the Co 3*d* states make great contribution to the magnetism of the Al_nCo^- clusters.

REFERENCES

1. *Wang H.Q., Kuang X.Y., Li H.F.* // Phys. Chem. Chem. Phys. – 2010. – **12**. – P. 5156.
2. *Li H.F., Kuang X.Y., Wang H.Q.* // Phys. Lett. A. – 2011. – **375**. – P. 2836.
3. *Reinhard P.G., Suraud E.* Introduction to Cluster Dynamics, Wiley-VCH, Weinheim, 2004.
4. *Baletto F., Ferrando R.* // Rev. Mod. Phys. – 2005. – **77**. – P. 371.
5. *Knickelbein M.B.* // Phys. Rev. Lett. – 2001. – **86**. – P. 5255.
6. *Gong X.G., Kumar V.* // Phys. Rev. B. – 1994. – **50**. – P. 17701.

7. *Li X., Wang L.S.* // Phys. Rev. B. – 2002. – **65**. – P. 153404-1.
8. *Leskiw B.D., Castleman A.W. Jr.* // Chem. Phys. Lett. – 2000. – **316**. – P. 31.
9. *Kiran B., Li X., Grubisic A., Gantefor G.F., Bowen K.H., Buurgert R., Schnockel H.* // Phys. Rev. Lett. – 2007. – **98**. – P. 256802.
10. *Rao B.K., Jena P.* // J. Chem. Phys. – 1999. – **111**. – P. 1890.
11. *Orlov A.O., Amlani I., Bernstein G.H.* // Science. – 1997. – **277**. – P. 928.
12. *Valden M., Lai X., Goodman D.W.* // Science. – 1998. – **281**. – P. 1647.
13. *Jones R.O.* // Phys. Rev. Lett. – 1991. – **67**. – P. 224.
14. *Jones R.O.* // J. Chem. Phys. – 1993. – **99**. – P. 1194.
15. *Yang S.H., Drabold D.A.* // Phys. Rev. B. – 1993. – **47**. – P. 1567.
16. *Rao B.K., Jena P.* // J. Chem. Hys. – 1999. – **111**. – P. 1890.
17. *Bergeron D.E., Castleman A.W.* // Science. – 2004. – **304**. – P. 84.
18. (a) *Bauschlicher C.J., Partridge H.* // J. Chem. Phys. – 1987. – **86**. – P. 7007. (b) *Bauschlicher C.J., Barnes L.A.* // J. Phys. Chem. – 1989. – **93**. – P. 2932.
19. *Marti A.N., Vela A.* // Phys. Rev. B. – 1994. – **49**. – P. 17464.
20. *Marti A.N., Vela A., Salahub D.R.* // J. Quantum Chem. – 1997. – **63**. – P. 301.
21. *Cha C.Y., Gantefr G., Eberhardt W.* // J. Chem. Phys. – 1994. – **100**. – P. 995.
22. *Hettich R.L.* // J. Am. Chem. Soc. – 1989. – **111**. – P. 8582.
23. *Hanley L., Ruatta S., Anderson S.* // J. Chem. Phys. – 1987. – **87**. – P. 260.
24. *Jarrold M.F., Bower J.E., Kraus J.S.* // J. Chem. Phys. – 1987. – **86**. – P. 3876.
25. *Taylor K.J., Pettiett C.L.* // Chem. Phys. Lett. – 1988. – **152**. – P. 347.
26. *Li X., Wu H.B., Wang X.B., Wang L.S.* // Phys. Rev. Lett. – 1998. – **81**. – P. 1909.
27. *Knight W.D.* // Phys. Rev. Lett. – 1984. – **52**. – P. 2141.
28. *Chou M.Y., Cohen M.L.* // Phys. Lett. A. – 1986. – **113**. – P. 420.
29. *Reddy B.V., Khanna S.N., Deevi S.C.* // Chem. Phys. Lett. – 2001. – **333**. – P. 465.
30. *Owen C.T., Zheng W.J., Bowen K. Jr.* // J. Chem. Phys. – 2001. – **114**. – P. 5514.
31. *Khanna S.N., Ashman C., Rao B.K., Jena P.* // J. Chem. Phys. – 2001. – **114**. – P. 9792.
32. *Gong X.G., Kumar V.* // Phys. Rev. Lett. – 1993. – **70**. – P. 2078.
33. *Bailey M.S., Wilson N.T.* // Eur. Phys. J.D. – 2003. – **25**. – P. 41.
34. *Lv J., Zhang F.Q., Jia J.F., Xu X.H., Wu H.S.* // J. Mol. Struct.: THEOCHEM. – 2010. – **955**. – P. 14.
35. *Wang M., Huang X.Y., Du Z.L., Li Y.C.* // Chem. Phys. Lett. – 2009. – **480**. – P. 258.
36. *Lim D.H., Negreira A.S., Wilcox J.* // J. Phys. Chem. C. – 2011. – **115**. – P. 8961.
37. *Nonose S., Sone Y., Onodera K., Sudo S., Kaya K.* // Chem. Phys. Lett. – 1989. – **164**. – P. 427.
38. *Menezes W.J.C., Knickelbein M.B.* // Chem. Phys. Lett. – 1991. – **183**. – P. 357.
39. *Menezes W.J.C., Knickelbein M.B.* // Z. Phys. D: Atom. Mol. Clust. – 1993. – **26**. – P. 322.
40. *Behm J.M., Brugh D.J., Morse M.D.* // J. Chem. Phys. – 1994. – **101**. – P. 6487.
41. *Kung X., Wang X., Liu G.* // J. Struct. Chem. – 2011. – **52**. – P. 675.
42. *Kozinkn A.V., Vlasenko V.G., Kulikova O.V., Shvachko O.V., Kozinkin Yu.A., Vysochina L.L., Guterman V.E., Znbavichus Ya.V.* // J. Struct. Chem . – 2011. – **52**. – P. 76.
43. *Ma G., Guo L.* // J. Struct. Chem. – 2012. – **53**. – P. 39.
44. *Pramann A., Nakajima A., Kata K.* // J.Chem. Phys. – 2001. – **115**. – P. 5404.
45. *Guo L.* // J. Alloys, Compounds. – 2008. – **466**. – P. 463.
46. *Becke A.D.* // Phys. Rev. A. – 1988. – **38**. – P. 3098.
47. *Perdew J.P., Wang Y.* // Phys. Rev. B. – 1992. – **45**. – P. 13244.
48. *Huber K.P., Herzberg G.* Constants of Diatomic Molecules, Molecular Spectra, Molecular Structure, vol. 4, Van Nostrand Rienhold. – New York, 1979.
49. *Kant A., Strauss B.* // J. Chem. Phys. – 1964. – **41**. – P. 3806.
50. *Hales D.A., Su C.X., Armenttrout P.B.* // J. Chem. Phys. – 1994. – **100**. – P. 1049.
51. *Ma Q.M., Xie Z., Wang J., Liu Y., Li Y.C.* // Phys. Lett. A. – 2006. – **358**. – P. 289.
52. *Sun J., Lu W.K., Wang H., Li Z.S., Sun C.C.* // J. Phys. Chem. A. – 2006. – **110**. – P. 2729.
53. *Reed A.E., Weinstock R.B., Weinhold F.* // J. Chem. Phys. – 1985. – **83**. – P. 735.
54. *Reed A.E., Curtiss L.A., Weinhold F.* // Chem. Rev. – 1988. – **88**. – P. 899.